JACS
JOURNAL OF THE AMERICAN CHEMICAL SOCIETY

Communication

pubs.acs.org/JACS

Dimensional Reduction of a Layered Metal Chalcogenide into a 1D Near-IR Direct Band Gap Semiconductor

Yi-Hsin Liu, Spencer H. Porter, and Joshua E. Goldberger*

Department of Chemistry and Biochemistry, The Ohio State University, Columbus, Ohio 43210-1340, United States

Supporting Information

ABSTRACT: Reducing the dimensionality of inorganic lattices allows for the creation of new materials that have unique optoelectronic properties. We demonstrate that a layered metal chalcogenide lattice, TiS_2, can form a dimensionally reduced crystalline one-dimensional hybrid organic/inorganic TiS_2(ethylenediamine) framework when synthesized from molecular precursors in solution. This solid has strong absorption above 1.70 eV and pronounced emission in the near-IR regime. The energy dependence of the absorption, the near-IR photoluminescence, and electronic band structure calculations confirm that TiS_2(ethylenediamine) has a direct band gap.

Layered two-dimensional (2D) metal chalcogenides have attracted considerable interest in the materials research community because of the wealth of interesting physical phenomena[1] and applications such as charge density waves,[2] superconductors,[3] topological insulators,[4] thermoelectric materials,[5] transistors,[6] and battery materials.[7] Dimensionally reduced hybrid organic/inorganic crystalline phases, that is, phases in which the framework connectivity of an inorganic crystal structure is partially disrupted along two or one dimensions through the coordination of an organic ligand, often exhibit unique and unexpected properties.[8] For example, it has been shown that the intrinisically three-dimensional sphalerite or wurtzite lattices, such as ZnS, ZnSe, and ZnTe, can be converted into atomically thin 2D and one-dimensional (1D) crystalline frameworks when synthesized via solution-phase techniques in the presence of alkylamine ligands.[8d,9] These materials show significantly enhanced band-edge absorptions and band gap tunabilities due to strong quantum-confinement effects[10] as well as reduced thermal conductivites,[9] making them of considerable interest for optoelectronic and thermoelectric applications.[11] These unique properties often arise from a synergistic combination of the excellent electromagnetic properties of the inorganic framework and the flexible, electronically insulating behavior of the organic ligand. Herein we demonstrate for the first time the dimensional reduction of a layered metal chalcogenide, TiS_2, into a hybrid 1D framework [TiS_2(en)] (en = ethylenediamine) composed of edge-sharing octahedral chains. Dimensional reduction significantly changes the narrow indirect band gap of bulk TiS_2 (0.3 eV),[12] converting this material into a direct band gap semiconductor (1.70 eV) that exhibits near-IR (NIR) photoluminescence.

We synthesized TiS_2(en) by the reaction of $TiCl_4$ with elemental sulfur that was dissolved in excess ethylenediamine at room temperature in a N_2 atmosphere, followed by annealing at 220 °C for 3−5 days in a Parr reactor (Scheme 1). TiS_2(en) formed upon subsequent addition of isopropanol. Scanning electron microscopy (SEM) showed that TiS_2(en) crystallized into jet-black, rodlike crystals that had an average diameter of 400 ± 200 nm and an average length of 1.5 ± 0.5 μm (Figure 1a). Elemental analysis confirmed the Ti:S:N:C:H stoichiometry of 1:2:2:2:8. This material is thermally stable up to 200 °C in nitrogen and stable in air for a couple of weeks.

Scheme 1. Reaction Pathway for Formation of TiS_2(en)

$$TiCl_4 + 2S + en \xrightarrow[2.\ i\text{-PrOH}]{1.\ 220\ ^\circ C} TiS_2(en)$$

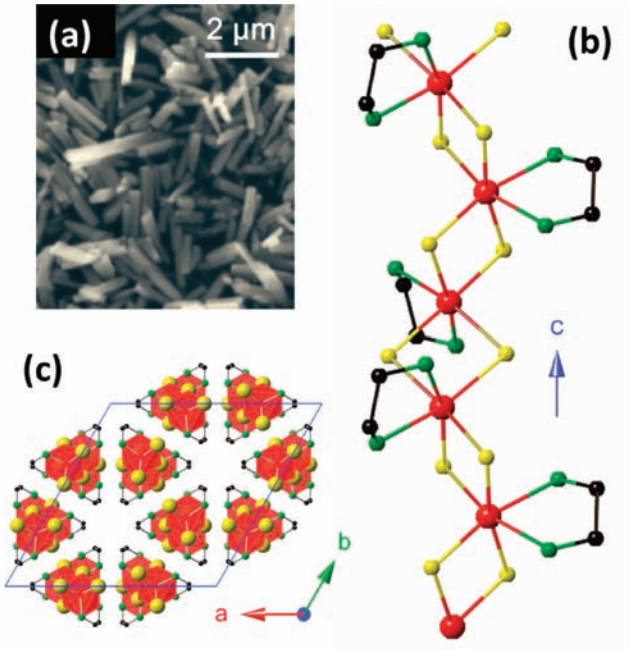

Figure 1. (a) SEM image of rodlike TiS_2(en) crystals. (b) Infinite TiS_2(en) chain along *c* axis. Atom colors: Ti, red; S, yellow; N, green; C, black. H atoms have been omitted for clarity. (c) View of TiS_2(en) projected down the *c* axis. Ti octahedra are shaded in orange.

Received: December 16, 2011
Published: February 24, 2012

   dx.doi.org/10.1021/ja211765y | *J. Am. Chem. Soc.* 2012, 134, 5044−5047

This phase has a trigonal unit cell [$a = b = 18.596(1)$ Å and $c = 9.0158(1)$ Å] with the $R\bar{3}c$ space group, as determined via Rietveld refinement of the synchrotron powder X-ray diffraction (XRD) pattern [Figure SI-1 in the Supporting Information (SI)]. The crystal structure consists of 1D edge-sharing chains of Ti octahedra in which each Ti atom is coordinated by four S atoms and two N atoms from a bidentate en ligand (Figure 1b). The bond angles of these octahedra are distorted away from ideal octahedral symmetry (Table S1 in the SI). Each octahedron is linked to its neighbors via two bridging S atoms in an edge-sharing fashion. The bidentate en ligand is rotated 120° for each neighboring octahedron along the chain axis, giving each chain a threefold helicity. In the unit cell, these chains pack into a hexagonal arrangement in which the carbon atoms of the en ligands are oriented into the void space between six neighboring chains, as evidenced by a view along the c axis of the unit cell (Figure 1c). The staggered conformation of ethylenediamine in this crystal structure was further confirmed via Raman spectroscopy (Figure SI-2). The changes in Ti–S and Ti–N bond lengths and vibrational frequencies due to coordination were confirmed via Raman spectroscopy and extended X-ray absorption fine structure (EXAFS) measurements (Figures SI-2 and SI-3).

This structure can be thought of as a distorted, dimensionally reduced derivative of the layered TiS_2 lattice. In the TiS_2 lattice, each layer consists of TiS_2 octahedra that share edges with six neighbors (Figure 2, left). A single chain of edge sharing Ti–S

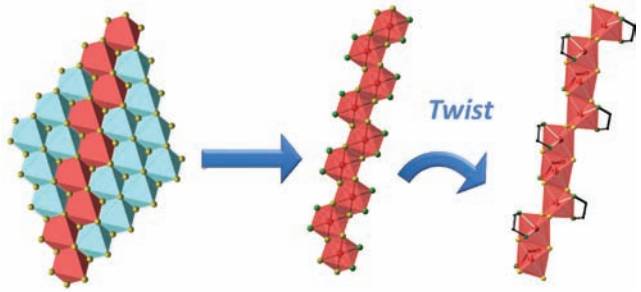

Figure 2. Schematic illustration of dimensional reduction of a single layer of TiS_2 (left), in which a 1D chain of edge-sharing octahedra is extracted (middle) and then the non-edge-sharing S atoms are replaced with en and the chain is twisted to form TiS_2(en) (right).

octahedra can be selected, such that four of the six neighboring Ti–S octahedra can be removed. This leaves on each Ti–S octahedron two nonedge-sharing S atoms, which are substituted with a bidentate en ligand. TiS_2(en) structure is derived by twisting each chain to achieve 3-fold helicity along each chain (Figure 1c, 2 right).

The optical properties of TiS_2(en) were investigated by both diffuse-reflectance absorption (DRA) spectrometry and photoluminescence measurements. The jet-black material has a broad absorption over visible wavelengths with an absorption onset at NIR wavelengths (Figure 3a). The band gap energy (E_g) was determined to be 1.708 eV by fitting the absorption edge to the Tauc/Davis–Mott expression $(h\nu\alpha)^{1/n} = A(h\nu - E_g)$, where $n = 0.5$ for a direct-band-gap material, A is a constant, $h\nu$ is the photon energy, and α is the absorption coefficient determined from the Kubelka–Munk function (Figure 3b). The linear relationship between $(h\nu\alpha)^2$ and the energy at the absorption onset, as shown in Figure 3a, is indicative of a direct band gap material. This 1.4 eV increase in the band gap in going from

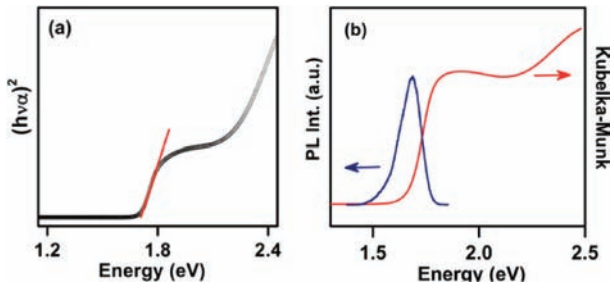

Figure 3. (a) DRA absorption spectrum of TiS_2(en) plotted as $(h\nu\alpha)^2$ vs photon energy, showing an estimated band gap of 1.70 eV. (b) Kubelka–Munk function optical absorption (red) and NIR photoluminescence of TiS_2(en) using 1.96 eV excitation energy (blue).

bulk TiS_2 to TiS_2(en) reflects the significant change in the band structure due to the reduced dimensionality.

A pronounced NIR photoluminescence was observed from both dried solid powder pellets and suspensions of micrometer particles in a variety of solvents, including isopropanol and dimethylformamide, at room temperature (Figure 3b). For both dispersed particles and the solid-state pellets, the photoluminescence was centered at 1.68 eV, which is 28 meV below the absorption band edge and indicative of band gap photoluminescence arising from a direct band gap material. The photoluminescence was independent of the excitation wavelength. The full width at half-maximum of this emission feature was ~0.12 eV. A more detailed spectroscopic study with lifetime, quantum yield, and temperature dependent measurements is currently underway.

To investigate the electronic structure of TiS_2(en), band-structure simulations were performed using density functional theory (DFT) as implemented in the Cambridge Serial Total Energy Package. The band structure calculations for this trigonal lattice were performed using the reduced rhombohedral unit cell and calculated along the RHL_2 **k**-space pathway of the Brillouin zone (Figure SI-4).[13] From these calculations, both the conduction band minimum and the valence band maximum were calculated to occur at the Γ point (Figure 4a).

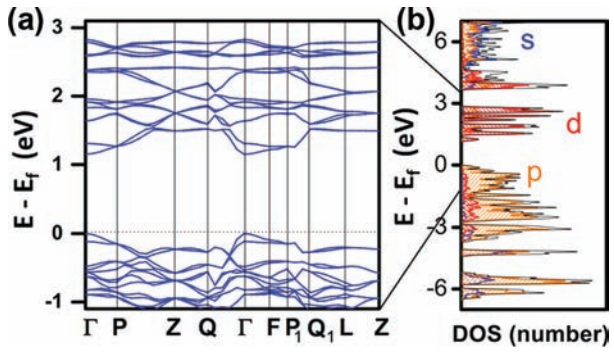

Figure 4. (a) Local electronic band structure for TiS_2(en). (b) Partial density of states, where s (red), p (blue), and d (orange) orbital contributions are summed (black).

The partial density of states (PDOS) for each orbital is plotted in Figure 4b and for each atom in (Figure SI-5). The atom-specific PDOS plots show the valence band maximum to be composed predominantly of S 3p orbitals; the N 2p orbitals lie 3 eV lower than the valence band maximum (Figure SI-5). The conduction band minimum is composed mainly of unoccupied Ti 3d orbitals and is split into lower energy bands comprised of

dx.doi.org/10.1021/ja211765y | J. Am. Chem. Soc. 2012, 134, 5044–5047

three d orbitals for each Ti atom (1.1−3 eV) and higher-energy bands comprised of two d orbitals for each Ti atom (3.7−4.5 eV). However, the distortion away from ideal octahedral symmetry further splits the degeneracy of these d orbitals. The calculated band gap energy was observed to be 1.1 eV, which is ∼35% lower than the absorption band edge. It is well-known that these simulations tend to underestimate the band gap by 30−40%.[14] Therefore, the simulated band-gap energy is in close agreement with the observed experimental data and further indicates that TiS_2(en) has a direct band gap in the NIR region. In previous studies, either the 1D metal chalcogenide structures (molecular wires) were metallic (e.g., $Li_xMo_6Se_6$,[15] Ag,[16] and Au nanowires[17]) or photoluminescent behavior was not reported.[18]

The change from indirect to direct band gap can be understood through a comparison of the band structures of TiS_2 and TiS_2(en). From DFT simulations of the band structure of TiS_2, the valence band maximum (derived mostly from S 3p orbitals) occurs at the Γ point, and the conduction band minima (consisting mainly of Ti 3d t_{2g} orbitals) in the M, A, and L directions are all lower in energy than at the Γ point (Figure SI-7a). From ARPES measurements on TiS_2 it has been established that the M point is the actual conduction band minimum, and most DFT simulations predict the energies of the A and L conduction band minima of TiS_2 to be too low.[12a,c] At the conduction band minimum in the M direction of TiS_2, each Ti atom has a 3d orbital of which two lobes having the same phase point directly at two of its edge-sharing Ti neighbors, resulting in a strong σ interaction, while the other two lobes having the opposite phase point away from its remaining four Ti neighbors (Figure SI-8).[19] The zigzag connectivity of the edge-sharing octahedra in the dimensionally reduced TiS_2(en) eliminates this low energy orbital configuration. The conduction band minima in the A and L Brillouin zone directions in TiS_2 are significantly influenced by interlayer coupling. In the 1D TiS_2(en) structure, the van der Waals gap between chains is 3.0 Å, compared with 2.7 Å for TiS_2, so the dispersion due to interlayer coupling is significantly weakened. Thus, the direct band gap in TiS_2(en) arises from the zigzag octahedral connectivity and the reduced interlayer coupling.

The increase in the band gap in going from TiS_2 to TiS_2(en) is a consequence of bandwidth narrowing in the dimensionally reduced crystal structure as well as the ligand substitution from S to N. To determine the influence of these two effects, we performed DFT simulations of a hypothetical structure in which the en of TiS_2(en) is replaced with a 1,2-ethanedithiol (et) linker (Figure SI-7b). This TiS_2(et) structure had the same space group and orientation as the original TiS_2(en) lattice. TiS_2(et) had a calculated direct band gap of 0.68 eV, which is smaller than the 1.1 eV band gap of TiS_2(en). The decrease in the band gap in going from TiS_2(en) to TiS_2(et) mainly arises from the increased dispersion of the valence-band maximum when the more electronegative and smaller N atoms on the ligand are substituted with the less electronegative and larger S atoms. Still, the conduction and valence band widths are significantly narrower in the TiS_2(et) and TiS_2(en) band structures than in TiS_2. Therefore, the reduced framework connectivity and change in crystal structure of the 1D TiS_2(en) system has a greater influence than ligand substitution in increasing the band gap of TiS_2. This 1−2 eV blue shift of the band gap has been commonly observed in many other dimensionally reduced hybrids.[20]

In summary, we have successfully synthesized the first dimensionally reduced 1D lattice of a layered metal chalcogenide using a solution-based technique. This TiS_2(en) structure consists of edge-sharing Ti−S octahedra that form 1D chains, which are isolated by an electronically insulating, coordinated en ligand. The resulting TiS_2(en) material has a direct band gap of 1.70 eV and exhibits NIR photoluminescence, making this a promising candidate for numerous optoelectronic applications. This structure opens up new opportunities for the design of hybrid organic/inorganic 1D materials from 2D metal chalcogenide structures via dimensional reduction.

■ ASSOCIATED CONTENT

Ⓢ Supporting Information

Experimental details and characterization data, including Raman, EXAFS, PDOS, and Brillion zone. This material is available free of charge via the Internet at http://pubs.acs.org.

■ AUTHOR INFORMATION

Corresponding Author

goldberger@chemistry.ohio-state.edu

Notes

The authors declare no competing financial interest.

■ ACKNOWLEDGMENTS

We acknowledge M. Suchomel (11-BM) and Q. Ma (5-BM-D) for the assistance in collecting XRD and EXAFS at the Advanced Photon Source at Argonne National Laboratory, which is supported by the U.S. Department of Energy, Office of Science, Office of Basic Energy Sciences, under Contract DE-AC02-06CH11357, and the Raman Spectroscopy Facility of the OSU Chemistry Department, which is supported by the National Science Foundation under Grant CHE-0639163. We also thank G. Natu, Z. Ji, and Prof. Y. Wu for NIR spectroscopy measurements and Prof. P. Woodward for helpful discussions. J.G. thanks the OSU Research Foundation for financial support.

■ REFERENCES

(1) Yoffe, A. D. *Adv. Phys.* **2002**, *51*, 799.

(2) Clerc, F.; Battaglia, C.; Cercellier, H.; Monney, C.; Berger, H.; Despont, L.; Garnier, M. G.; Aebi, P. *J. Phys.: Condens. Matter* **2007**, *19*, No. 355002.

(3) Gamble, F. R.; Silbernagel, B. G. *J. Chem. Phys.* **1975**, *63*, 2544.

(4) Xu, S.-Y.; Xia, Y.; Wray, L. A.; Jia, S.; Meier, F.; Dil, J. H.; Osterwalder, J.; Slomski, B.; Bansil, A.; Lin, H.; Cava, R. J.; Hasan, M. Z. *Science* **2011**, *332*, 560.

(5) (a) Amara, A.; Frongillo, Y.; Aubin, M. J.; Jandl, S.; Lopez-Castillo, J. M.; Jay-Gerin, J. P. *Phys. Rev. B* **1987**, *36*, 6415. (b) Chung, D.-Y.; Hogan, T.; Brazis, P.; Rocci-Lane, M.; Kannewurf, C.; Bastea, M.; Uher, C.; Kanatzidis, M. G. *Science* **2000**, *287*, 1024.

(6) Radisavljevic, B.; Radenovic, A.; Brivio, J.; Giacometti, V.; Kis, A. *Nat. Nanotechnol.* **2011**, *6*, 147.

(7) (a) Whittingham, M. S. *Chem. Rev.* **2004**, *104*, 4271. (b) Whittingham, M. S. *Science* **1976**, *192*, 1126.

(8) (a) Mitzi, D. B. *Adv. Mater.* **2009**, *21*, 3141. (b) Long, J. R.; McCarty, L. S.; Holm, R. H. *J. Am. Chem. Soc.* **1996**, *118*, 4603. (c) Kagan, C. R.; Mitzi, D. B.; Dimitrakopoulos, C. D. *Science* **1999**, *286*, 945. (d) Huang, X.; Li, J.; Fu, H. *J. Am. Chem. Soc.* **2000**, *122*, 8789.

(9) Huang, X.; Roushan, M.; Emge, T. J.; Bi, W.; Thiagarajan, S.; Cheng, J.-H.; Yang, R.; Li, J. *Angew. Chem., Int. Ed.* **2009**, *48*, 7871.

(10) Buhro, W. E.; Colvin, V. L. *Nat. Mater.* **2003**, *2*, 138.

(11) Mishra, S. K.; Satpathy, S.; Jepsen, O. *J. Phys.: Condens. Matter* **1997**, *9*, 461.

(12) (a) Chen, C. H.; Fabian, W.; Brown, F. C.; Woo, K. C.; Davies, B.; DeLong, B.; Thompson, A. H. *Phys. Rev. B* **1980**, *21*, 615. (b) Myron, H. W.; Freeman, A. J. *Phys. Rev. B* **1974**, *9*, 481. (c) Fang, C. M.; de Groot, R. A.; Haas, C. *Phys. Rev. B* **1997**, *56*, 4455.

(13) Setyawan, W.; Curtarolo, S. *Comput. Mater. Sci.* **2010**, *49*, 299.
(14) (a) Sham, L. J.; Schlüter, M. *Phys. Rev. B* **1985**, *32*, 3883. (b) Sun, J.; Buhro, W. E.; Wang, L.-W.; Schrier, J. *Nano Lett.* **2008**, *8*, 2913. (c) Seidl, A.; Görling, A.; Vogl, P.; Majewski, J. A.; Levy, M. *Phys. Rev. B* **1996**, *53*, 3764.
(15) Venkataraman, L.; Lieber, C. M. *Phys. Rev. Lett.* **1999**, *83*, 5334.
(16) Hong, B. H.; Bae, S. C.; Lee, C.-W.; Jeong, S.; Kim, K. S. *Science* **2001**, *294*, 348.
(17) (a) Huo, Z.; Tsung, C.-k.; Huang, W.; Zhang, X.; Yang, P. *Nano Lett.* **2008**, *8*, 2041. (b) Lu, X.; Yavuz, M. S.; Tuan, H.-Y.; Korgel, B. A.; Xia, Y. *J. Am. Chem. Soc.* **2008**, *130*, 8900.
(18) Campbell, M. G.; Powers, D. C.; Raynaud, J.; Graham, M. J.; Xie, P.; Lee, E.; Ritter, T. *Nat. Chem.* **2011**, *3*, 949.
(19) Wilson, J. A.; Yoffe, A. D. *Adv. Phys.* **1969**, *18*, 193.
(20) (a) Fluegel, B.; Zhang, Y.; Mascarenhas, A.; Huang, X.; Li, J. *Phys. Rev. B* **2004**, *70*, No. 205308. (b) Huang, X.; Li, J. *J. Am. Chem. Soc.* **2007**, *129*, 3157. (c) Walsh, A. *Proc. R. Soc. A* **2011**, *467*, 1970.